Real-Time Implementation of Cascade Nonlinear FF-PI Retarted Controller Design for Industrial Process Systems

Kagan Koray Ayten *, Ahmet Dumlu, Sadrettin Golcugezli, Emre Tusik, Gurkan Kalınay

Posted Date: 5 August 2024

doi: 10.20944/preprints202408.0288.v1

Keywords: cascade control; time delayed system; time delayed control; CPIR control; CNPIR control; FF-PI control; coupled tank liquid level control; dynamic

Article

Real-Time Implementation of Cascade Nonlinear FF-PI Retarted Controller Design for Industrial Process Systems

Kagan Koray Ayten [1,*], Ahmet Dumlu [1], Sadrettin Golcugezli [2], Emre Tusik [1] and Gurkan Kalınay [1]

[1] Department of Electrical & Electronic Engineering, Erzurum Technical University, Erzurum 25550, Turkiye; kagan.koray@erzurum.edu.tr (K.K.A.); ahmetdumlu@erzurum.edu.tr (A.D.); gurkan.kalinay@erzurum.edu.tr (G.K); emre.tusik@erzurum.edu.tr (E.T);

[2] Department of Electrical & Electronic Engineering, Ataturk University, Erzurum 25550,Turkiye; sadrettin.golcugezli@atauni.edu.tr (S.G);

* Correspondence: kagan.koray@erzurum.edu.tr

Abstract: This study introduces a cascade nonlinear proportional integral retarded (CNPIR) controller for the first time in the literature, aiming to achieve real-time precise control of a double-tank liquid level system. It begins by outlining the characteristics of delay-based systems and detailing the dynamic behavior of the liquid-level system. The study evaluates the system's performance by developing and analyzing the mathematical models of both the feedforward proportional-integral (FF-PI) controller and the CNPIR controller. Two different control techniques were employed, with real-time tests conducted to assess the system's axis movement performance. The FF-PI controller was used as the initial control technique, while the CNPIR controller was introduced to enhance system performance during trajectory tracking. Experimental results demonstrated that the CNPIR method significantly improved trajectory tracking response, reduced overshoot, and achieved better steady-state error under external disturbances compared to the FF-PI controller. Thus, the experimental study, highlights the effectiveness of the proposed control design and its superiority over some existing classical methods.

Keywords: cascade control; time delayed system; time delayed control; CPIR control; CNPIR control; FF-PI control; coupled tank liquid level control; dynamic

1. Introduction

Time delay, also known as "dead time" in automatic control theory, determines the impact of a reference signal on a control system's output after a specific duration. This is an inevitable situation in many control systems that operate in real time. A time delay in a control system can be caused by the sensors present in the system, the internal structure of the system, or the complexity with which the controller is designed. There are two different methods to evaluate this effect. The first method involves verbally discussing the control mechanisms, the control controller, and the time delay. The second and most important methodology is to calculate and analyse how time delays affect control mechanisms. For this reason, many studies have been carried out in the literature to mathematically explain the effect of time delay in control systems, and many different approaches have been developed about its mathematical analysis and effects. The characteristic equation of a closed-loop control system is written as a quasi-polynomial instead of a polynomial when there is a time delay in the control system algorithm. Polynomials have a finite number of roots, while polynomial equations have an infinite number of roots. This feature is one of the most important differences that separates the two characteristic structures. Given that the system's behaviour heavily depends on the positions of the closed loop poles, the system's time delay complicates both its analysis and its design. The Hermite-Biehler theorem, the Nyquist theorem, and the Walton-Marshall direct method are the most

 doi:10.20944/preprints202408.0288.v1

often used techniques in the literature for determining the stability of time-delayed control systems. The Hermite-Biehler Theorem, with its generalized version for polynomials, is unique among these techniques [1]. The Nyquist theorem has served as the foundation for numerous investigations [2,3]. Numerous investigations have demonstrated the efficacy and power of the Walton-Marshall direct technique in determining the stability of control systems with time delays. Compared to the Nyquist theorem and the Hermite-Biehler theorem, this method is faster and more convenient. Furthermore, this method provides valuable insights into the effects of time delays on the number of poles in the right half s plane of an unstable control system and how this number may vary [4]. The literature has conducted numerous studies on time-delay control designs. One of the studies on this subject focused on frequency shaping by taking advantage of the stabilizing properties of time delays [5]. Another study proposed a new controller type that leverages the time delay effect [6]. It has been stated that this control structure can replace the PD controller by performing a mean derivative action. The traditional P controller, equipped with a suitable time delay, provides fast responses to input changes and is insensitive to high-frequency noise. Researchers conducted a study to stabilize oscillatory systems, demonstrating that positive, delayed feedback stabilized the oscillatory system [7]. This study demonstrates the stability of the closed-loop system using the Nyquist criterion across various delays. In another study on time-delayed systems in the literature, Niculescu and Michiels showed that time delay provides stabilization of linear systems, including integrator chains [8]. Galip Ulusoy proposed a time-delayed control structure for single-input, single-output linear time-invariant systems [9]. This control structure is known to enhance stability margins and decrease sensitivity. Another study demonstrated that the cascade control network enhances the control mechanism's performance, particularly when faced with unpredictable disturbances [10]. The stability of the control system is improved in this study by using the cascade controller algorithm in a single machine power system that is linked to an infinite busbar that has a Static Synchronous Series Compensator (SSSC). The cascade control method has proven to perform better than standard control methods. The literature contains numerous studies on control of dual tank systems, a type of time-delayed system. The first of the recent studies is the adaptive-based control technique, which is especially sensitive to disturbances [11]. The adaptable feature of the controller parameters in this study enabled excellent control performance, even in the face of undetermined system parameters and disturbances. The fractional order controller design is another control method [12]. In this liquid level control study, system performance was increased by using a fractional order PI controller instead of the classical PI controller. Another study in the literature used the backstepping controller and the developed observer effect to prevent disruptive effects from occurring in the system [13]. Additionally, researchers tested the system's performance by applying control techniques such as fuzzy logic-based PI control [14] and genetic algorithm-based tuneable artificial neural network control [15].

Another study used a control design to control a time-delayed double tank system in real time. This control design is known as a cascade proportional integral retarded (CPIR) controller. Initially, López built and tested this controller for DC servo motor position control [16]. The suggested controller features an outer loop and an inner loop in a stepwise configuration. The inner loop, with its delayed algorithm structure, adjusts the angular velocity of the regulated DC servo motor, while the outer loop uses a proportional controller to modify the system's angular position. This controller has been able to achieve excellent position control under varying loads and disruptive effects, as well as eliminating overshoots that may occur during position changes. It is capable of monitoring the DC servo motor's angular velocity without the need for extra filters.

Different research suggests utilizing a fractional IMC filter PID control approach to improve the efficiency of cascade control systems that are frequently employed in chemical process industries [17]. The suggested method enhances control performance, particularly in set point tracking, disturbance rejection, and noise handling, by incorporating a fractional order filter in the outer loop and completing thorough robustness and fragility evaluations. The study used an analytical methodology to create and fine-tune the controllers, streamlining the whole design process and reducing errors. The versatility of the fractional IMC filter and its ability to be applied to different process models demonstrate its potential for widespread industrial utilization.

 doi:10.20944/preprints202408.0288.v1

A simple and effective control strategy for time-delayed unstable series cascade processes is also given in [18]. By utilizing a PID controller with a second-order lead-lag filter in conjunction with an IMC controller, the proposed method simplifies the control design while ensuring robust performance and efficient disturbance rejection. The innovative use of an underdamped IMC filter configuration enhances the reset rate action, providing improved integral performance. Despite its advantages, the strategy's applicability to more complex or different types of processes remains limited, and its reliance on accurate process modelling is a potential drawback. Simulation studies validate the method's efficacy, but real-world testing is needed for a comprehensive evaluation.

A robust and efficient control strategy for unstable processes with time delay, leveraging a modified Smith predictor in a cascade control structure, was introduced in [19]. While it simplifies controller design and enhances performance, especially in disturbance rejection and robustness, the practical implementation may still pose challenges and require careful handling of process model accuracy and overshoot issues.

Another paper underscores the limitations of conventional PI control in CAV systems and highlights the potential of advanced control strategies, particularly model-based approaches, to improve system performance [20]. The proposed model-based cascade control method is positioned as a promising solution to overcome the challenges of thermal inertia and dynamic uncertainties in CAV air-conditioning systems, offering better control robustness and accuracy.

In [21], simulations on double tanks have demonstrated that the genetic fuzzy cascade control method offers rapid adjustment speed, minimal overshoot, and excellent stability, thereby enhancing the automation level of the liquid level control system. Consequently, this control method offers efficient control performance for systems characterized by an unstable transfer function and a pure time delay. A separate work introduces comprehensive autotuning parameters for 2-DOF PI/PID controllers in a cascade control setup [22]. The requirement for achieving the best possible performance in tracking and regulation modes has resulted in the adoption of the corresponding two degrees of freedom (2-DOF) version for the controllers. The autotuning algorithms for both the inner and outer loop controller parameters have effectively resolved the limitations associated with tuning a cascade control arrangement [23].

This study aimed to design a robust and efficient controller that could precisely control the liquid level system. This controller is made to be resilient and adaptable to unknown loads and the unmodeled and/or unmodelable dynamics of nonlinear systems. To overcome these mentioned conditions, a cascade nonlinear proportional integral retarded (CNPIR) control design was used for the first time in the literature to control a double-tank liquid level system in real-time. The specified cascade controller has been employed to enhance robustness against disturbances and noise that may occur during the system's operation. Additionally, a systematic approach utilizes this controller, which fundamentally incorporates a time delay, to enhance the system's ability to increase position and velocity tracking precision, simplify system modelling, and resolve stability maintenance issues. Furthermore, it possesses a control structure that enhances system performance for modelling instabilities. This feature of the CNPIR technique, in contrast to the classical PI control technique, restructures the dynamic equations of the system under control within a specific framework, enabling the generation of appropriate control signals during the system's movement. In this manner, the system minimizes position and velocity errors. Finding a full and accurate dynamic model of the system and using it, especially in the CNPIR control method, leads to better control performance than traditional PI control, according to the results.

The following is the work's outline: The FF-PI, CPIR, and CNPIR control laws are defined in the next section, which also addresses closed-loop liquid-level system modelling concerns. Several results are reported later in the section on experimental results. A few closing thoughts and a list of topics that warrant more research complete this work.

2. Dynamic Model of Liquid Level and System Description

Figure 1 depicts the closed recirculating test system used for a connected tank. The system comprises two interconnected liquid tanks, an electrically operated pump, a level monitoring

 doi:10.20944/preprints202408.0288.v1

aperture at the bottom of each tank, and a pressure sensor. Tank 1 is supplied by the electric pump, and Figure 1 shows how both liquid tanks are mounted on the front plate. Tank 2 receives the outflow from Tank 1. Two pressure-sensitive sensors, located at the base of each tank, measure the liquid levels in both reservoirs.

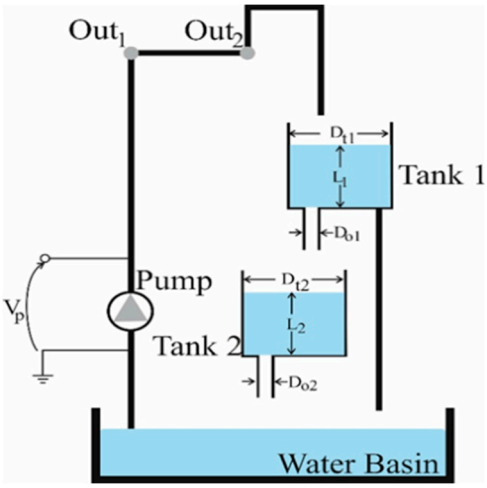

Figure 1. The coupled-tank recirculating system.

The mathematical basis of the interconnected tank system can be found in [24]. The rate of change of the liquid level in each separate reservoir is as follows:

$$\dot{L}_i(t) = \frac{1}{A_i}\left(F_{IN_i} - F_{OUT_i}\right) \quad i = 1,2 \tag{1}$$

The variable $L_i(t)$ represents the liquid level in the reservoir, measured in centimetres. A_i represents the cross-sectional area of the reservoir, measured in square centimeters. F_{IN_i} and F_{OUT_i} represent the inflow and outflow rates of the i-th tank, measured in cubic centimetres per second. The rate at which liquid flows into tank 1 is precisely proportional to the voltage that is applied to the pump. This means that as the voltage increases, the inflow rate into the tank also increases.

$$F_{IN_1} = K_p V_p(t) \tag{2}$$

The constant K_p represents the pump's conversion factor in cubic centimetres per volt-second (cm^3/Vs). The control input, $V_p(t)$, also known as the voltage pump $u(t)$ in volts ($Volt$), is utilized to attain the desired levels in either tank 1 or tank 2 as follows;

$$u(t) = u_1(t) + u_2(t) \tag{3}$$

The contributions of the cascade rule and the feedforward action are denoted by $u_1(t)$ *and* $u_2(t)$, respectively, in Equation (3). Moreover, Equation (4) provides the outflow velocity from the orifice at the bottom of each unique tank using Bernoulli's law.

$$v_{OUT_i}(t) = \sqrt{2gL_i(t)} \tag{4}$$

Next, using Equation (5), the outflow percentage of a separate liquid tank is calculated.

$$F_{OUT_i}(t) = a_i\sqrt{2gL_i(t)} \tag{5}$$

where a_i is the cross-sectional area of the outflow orifice (cm^2) at the bottom of the i-th tank, and g is the gravitational acceleration (981 cm/s^2). Tank 2's inflow is determined as follows;

$$F_{IN_2}(t) = F_{OUT_1}(t) \tag{6}$$

 doi:10.20944/preprints202408.0288.v1

Thus, the following mathematical expression for the liquid level in the connected tanks can be produced by applying the mass balance principle and Equations (1-6);

$$\dot{L}_1(t) = \frac{K_p u(t) - a_1\sqrt{2gL_1(t)}}{A_1} \tag{7}$$

$$\dot{L}_2(t) = \frac{a_1}{A_2}\sqrt{2gL_1(t)} - \frac{a_2}{A_2}\sqrt{2gL_2(t)} \tag{8}$$

The steady-state pump voltage, $u_1(t)$, that leads to the steady-state level, L_{10}, in reservoir 1 is determined by using Equation (7) when the system is at equilibrium ($\dot{L}_1(t) = 0$). Equation (8) is employed to determine the value of L_{10} in reservoir 1 when the system is at equilibrium ($\dot{L}_2(t) = 0$). This value represents the desired constant level in reservoir 2, referred to as the planned steady-state level. The relationships are specified in Equations (9) and (10).

$$u_1(t) = a_1\frac{\sqrt{2gL_{10}}}{K_p} \tag{9}$$

$$L_{10} = (\frac{a_2}{a_1})^2 L_{20} \tag{10}$$

Deviation variables can be defined by utilizing the operational range that corresponds to small departure voltages ($u_1(t)$) and heights ($L_1(t), L_2(t)$);

$$\begin{aligned} L_{11}(t) &= L_1(t) - L_{10} \\ L_{21}(t) &= L_2(t) - L_{20} \\ u_2(t) &= u(t) - u_1(t) \end{aligned} \tag{11}$$

The cascade control is denoted by $u_2(t)$. Thus, it is possible to translate the dynamic equations of Equation (7) and Equation (8) as follows:

$$\dot{L}_1(t) = -\frac{a_1}{A_1}\sqrt{2g(L_{10} + L_{11}(t))} + \frac{K_p}{A_1}(u_1(t) + u_2(t)) \tag{12}$$

$$\dot{L}_2(t) = -\frac{a_1}{A_2}\sqrt{2g(L_{11}(t) + L_{10})} - \frac{a_2}{A_2}\sqrt{2g(L_{21}(t) + L_{20})} \tag{13}$$

The liquid level system's dynamic equations are nonlinear due to the characteristics of the pump and valve, as well as variations in the system's parameters, as shown by Equations (12) and (13). In order to execute the suggested cascade for the connected tank system, it is necessary to linearize the linked tank system model around the operational point $(L_{10}, u(t)) = (L_{10}, u_1(t))$. Applying the first-order Taylor series approximation at the points (L_{20}, L_{10} and $u_1(t)$) to Equations (12) and (13) results in the following:

$$\dot{L}_{11}(t) = \alpha_1 L_{11}(t) + \beta_1 u_2(t) \tag{14}$$

$$\dot{L}_{21}(t) = \alpha_2 L_{21}(t) + \beta_2 L_{11}(t) \tag{15}$$

where,

$$\alpha_1 \cong -\frac{a_1}{A_1}\sqrt{\frac{g}{2L_{10}}}, \qquad \beta_1 \cong \frac{K_p}{A_1} \tag{16}$$

 doi:10.20944/preprints202408.0288.v1

$$\alpha_2 \cong -\frac{a_2}{A_2}\sqrt{\frac{g}{2L_{20}}}, \qquad \beta_2 \cong \frac{a_1}{A_2}\sqrt{\frac{g}{2L_{10}}}$$

After analysing the subsystem decomposition of Equation (14) and Equation (15), the task of regulating the level in Tank 2 (i.e., achieving set-point control of $L_2(t)$) is established. In this particular context, L_{21} and L_{11} symbolize the output and input of the subsystem, respectively, as mentioned in Equation (15). In addition, the subsystems in Equations (14) and (15) are modelled as transfer functions, and the Laplace transforms of these equations are given in Equations (17) and (18) as follow;

$$G_1(s) = \frac{K_1}{\tau_1 s + 1} \tag{17}$$

$$G_2(s) = \frac{K_2}{\tau_2 s + 1} \tag{18}$$

where, $K_1 = \frac{K_p\sqrt{2gL_{10}}}{a_1 g}$, $K_2 = \frac{a_1\sqrt{L_{20}}}{a_2\sqrt{L_{10}}}$, $\tau_1 = \frac{A_1\sqrt{2gL_{10}}}{a_1 g}$ and $\tau_2 = \frac{A_2\sqrt{2gL_{20}}}{a_2 g}$. It is evident that Equations (17) and (18) can be applied to both cascade and traditional PI. Table 1 displays the parameters of the connected tank system.

Table 1. Liquid level system parameters.

Description	Symbol	Value & Unit
Constant of Pump Flow	K_p	3.3 $cm^3/s/V$
Gravitational constant	g	981 $\frac{cm}{s^2}$
Tank 1&2 Outlet Areas	$a_1 = a_2$	0.1781 cm^2
Tank 1&2 Inside Cross-Section Areas	$A_1 = A_2$	15.5179 cm^2

2.1. Controller Design

In this section, the liquid level system has been subjected to a classical PI controller design with feedforward application in order to provide real-time position control. In order to improve the accuracy of controlling the liquid level system, a controller design called cascade nonlinear proportional integral retarded (CNPIR) has been developed. This design takes into consideration the dynamic models of the system.

2.1.1. Feed-Forward Proportional Integral Controller Design (FF-PI) Tank 1

Feedforward action in process control technology counteracts the impact of the measured disturbance on the process output. In this situation, the feedforward action is used to counterbalance the water being taken out (due to gravity) through the orifices at the bottom outlets of Tank 1 and Tank 2. However, the effects of unaccounted dynamics and disturbances are addressed by the cascade proportional-integral controllers, which are designed to handle time delays. A control pump is specifically engineered to modulate the water level or elevation by means of electricity. The control structure at the beginning is a feedforward proportional-integral controller (FF-PI) as shown in Figure 2.

Preprints.org (www.preprints.org) | NOT PEER-REVIEWED | Posted: 5 August 2024 doi:10.20944/preprints202408.0288.v1

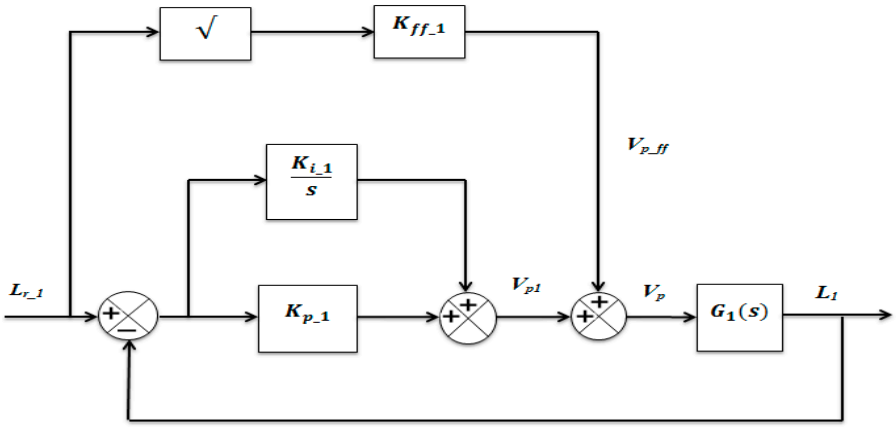

Figure 2. Feedforward PI control block diagram for Tank-1 experiment.

For zero steady-state error, the water level in Tank 1 is controlled through a positive proportional-integral (PI) closed-loop scheme with the addition of feedforward action, as shown in Figure 2. The mathematical equation for the voltage feedforward controller is presented in Equations (19) and (20) as follow;

$$V_{p_{ff}} = K_{ff_1}\sqrt{L_{r_1}} \tag{19}$$

$$V_p = V_{p1} + V_{p_{ff}} \tag{20}$$

While the feedforward action compensates for water withdrawal (due to gravity) through the bottom outlet of Tank 1, the PI controller compensates for dynamic disturbances. The transfer function of the feedforward PI control indicated in Figure 2 can be expressed as in Equation (21).

$$G_1(s) = \frac{L_1(s)}{V_{p1}(s)} \tag{21}$$

After conducting the liquid level experiment in Tank 1 with the feedforward PI controller, the CNPIR controller was used, considering the system dynamics. Thus, both control structures were compared through real-time experiments.

2.1.2. Feed-Forward Proportional Integral Controller Design (FF-PI) Tank 2

The second tank, which is designed with a feedforward proportional-integral controller, is shown in Figure 3. In the designed block diagram, the closed-loop transfer function, named $T_1(s)$, represents the water level of the 1st tank and is mathematically expressed in Equation (22) as follow;

$$T_1(s) = \frac{L_1(s)}{L_{r\_1}(s)} \tag{22}$$

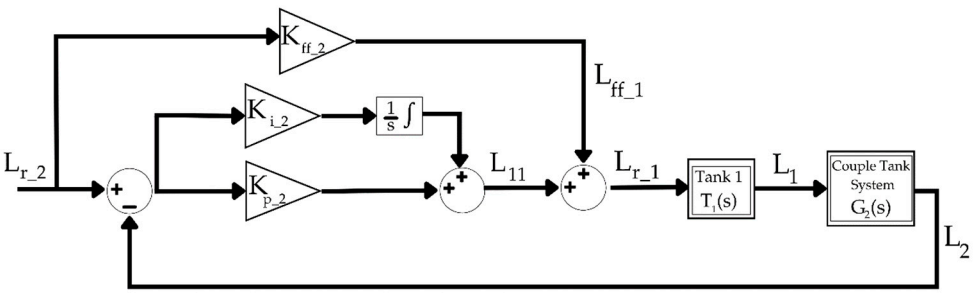

Figure 3. Feedforward PI control block diagram for Tank-2 experiment.

 doi:10.20944/preprints202408.0288.v1

The feedforward effect is mathematically expressed by the following Equation (23):

$$L_{ff\_1} = L_{r\_2} K_{ff\_2} \tag{23}$$

The input signal for the liquid level in Tank 1, L_{r_1}, is equal to the sum of L_{11}, which is called the small increase in liquid height calculated by the proportional-integral (PI) controller, and L_{ff_1}, which is obtained from the feedforward effect.

$$L_{r\_1} = L_{ff\_1} + L_{11} \tag{24}$$

According to Equation (24), the desired liquid level control of the tank is achieved as a result of the feedforward effect and the values calculated by the PI controller. To calculate the transfer function of Tank 2, the output value of Tank 2 needs to be divided by the input value of Tank 1 as follows;

$$G_2(s) = \frac{L_2(s)}{L_1(s)} \tag{25}$$

2.1.3. CPIR and CNPIR Controller Methods

In this section, the mathematical model and block structure of the time-delayed CPIR and CNPIR controllers are explained, considering the system dynamic model for the position control of the liquid level tank. Velocity measurements feed the Integral Retarded (IR) controller, which corresponds to the inner loop. Three parameters need to be adjusted: the gains K_i, K_{ir}, and the time delay h. The outer loop is closed using a proportional controller with a gain of K_p and is supplied with position readings. Equation (26) defines the time-effective mathematical expression of the CPIR controller [16].

$$\dot{u}(t) = (K_i - K_{ir})K_P e(t) + K_{ir}\dot{y}(t-h) - K_i\dot{y}(t) \tag{26}$$

Here, $\dot{y}(t)$ represents the derivative of the output parameter, in other words, the change in liquid level for Tank 1 and Tank 2. The characteristic quasi-polynomial of the closed-loop system is directly obtained with the help of Figure 3 and is presented in Equation (27). In Figure 3, the reference input y_d represents the desired liquid level for Tank 1 and Tank 2, while $y(t)$ represents the output magnitude, i.e., the liquid level obtained for Tank 1 and Tank 2.

$$p(s) = s^3 + as^2 + bK_i s + bK_p(K_i + K_{ir}) - bK_{ir}se^{-sh} \tag{27}$$

However, the quasi-polynomial expression of the inner velocity loop can be defined by Equation (28) as follow;

$$v(s) = s^2 + as + bK_i \pm bK_{ir}se^{-sh} \tag{28}$$

Figure 4 displays the closed-loop CNPIR controller. In this case, the CNPIR control law [16] can be defined in its most general form by Equation (29) as follows;

$$\dot{u}(t) = [(K_i - K_{ir})/G]SAT(GK_P e(t)) + K_{ir}\dot{y}(t-h) - K_i\dot{y}(t) \tag{29}$$

The saturation function of CNPIR is shown in Figure 4 and this function specified in Equation (29) is expressed by Equation (30) as follows;

$$SAT(x) = \begin{cases} x, & |x| \leq 1 \\ -1, & x < -1 \\ 1, & x > 1 \end{cases} \tag{30}$$

Preprints.org (www.preprints.org) | NOT PEER-REVIEWED | Posted: 5 August 2024 doi:10.20944/preprints202408.0288.v1

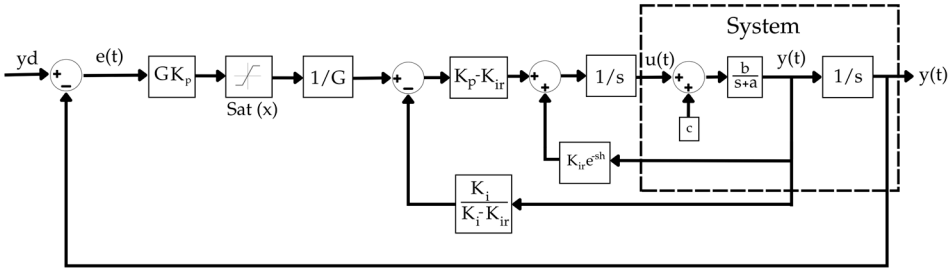

Figure 4. CNPIR controller block diagram.

Equation (29) defines $'G'$ as the scaling factor. If the positional error $e(t)$ is small enough, the value of $x = GK_P e(t)$ does not exceed the saturation limitations, and both the outer and inner loops operate in conjunction. Therefore, the values of G and $1/G$ nullify each other. If the positioning task results in a significant position error, $SAT(x)$ can be either 1 or -1. Here, the outer loop is disabled, and only the inner velocity loop functions. The system attains a steady velocity. When the position error diminishes, the saturation block functions within its linear range, causing both loops to become active once more. An advantage of the CPIR controller over the standard P-PI controller is its utilization of time delays, which effectively eliminates the need for velocity measurements. The second advantage is that the CPIR method does not use the finite differences method, thereby eliminating the deficiencies associated with high-pass filters. The initial design of the CPIR controller, which does not have a cascade structure, is called the Proportional Integral Retarded (PIR) controller. When a new outer loop is added to this PIR controller, the CPIR controller architecture is obtained. The CPIR controller has a notable advantage over the PIR controller in that the inner loop within the controller can function independently if the extra outer loop is disengaged. The addition of a saturation function (SAT) to the CPIR controller results in the formation of the Cascade Nonlinear Proportional Integral Retarded (CNPIR) controller design [16]. Incorporating the saturation function into the controller architecture offers a notable benefit, especially in terms of mitigating overshoot in the system's response. For more detailed information on the tuning methodology for CNPIR, see reference [16].

3. Experimental Results

The experimental system used in this study is shown in Figure 5. This system, produced by Quanser, operates with MATLAB Simulink. The necessary data for the system is obtained using the Quanser Q8 data acquisition card. For real-time position control experiments of the liquid level system, FF-PI and CNPIR controllers were implemented in the MATLAB-Simulink program, as shown in Figure 5. In the experiment, reference position changes were initially defined for both controller designs. These reference position changes were used to obtain error variations by comparing them with the liquid level in Tank 1 and Tank 2. These error variations were then provided as inputs to both controllers. Based on the mathematical equations defined according to the error variations, pump control signals were defined for the system. These control signals were applied directly to the system via the pump, and the liquid level changes were observed.

Preprints.org (www.preprints.org) | NOT PEER-REVIEWED | Posted: 5 August 2024 doi:10.20944/preprints202408.0288.v1

Figure 5. Quanser liquid level system where the experiments were carried out.

3.1. Results of Tank 1

Considering the system dynamics, the best parameter values for both controllers were provided to the system, and the control performances of the CNPIR and FF-PI controllers for Tank 1 were obtained as shown in Figure 6. In the experiments, the best controller parameters determined for Tank 1 are presented in Table 2. To achieve these optimal sensitivity parameters, simulation studies were first conducted. During the simulation studies, suitable parameter ranges were defined using a trial-and-error method. In real-time experiments, small variations were made to these parameters to obtain the optimal controller gain values.

Table 2. Liquid level system parameters.

FF-PI Parameters					
	K_{p_1} = 7.2152		K_{i_1} = 9.1061		K_{ff_1} = 2.391
CNPIR Control Parameters					
Square Wave	G= 0.442	h=0.002	K_p= 0.88	K_i= 26	K_{ir}= 0.01

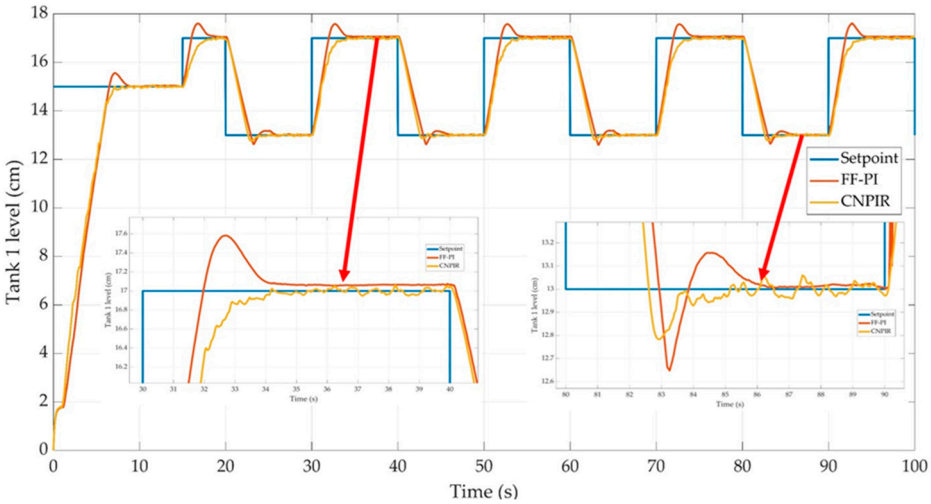

Figure 6. Control performances of the CNPIR and FF-PI controllers for Tank 1.

 doi:10.20944/preprints202408.0288.v1

The error of the Tank 1 level in the real-time process can be described as the discrepancy between the provided reference and the actual measured trajectory. In Figure 7, the square wave reference exhibits a minimal error percentage for the suggested CNPIR method, while the step reference shows a maximum error percentage of around 3.7% for the FF-PI method. In CNPIR, the maximum exceedance error value is negligible.

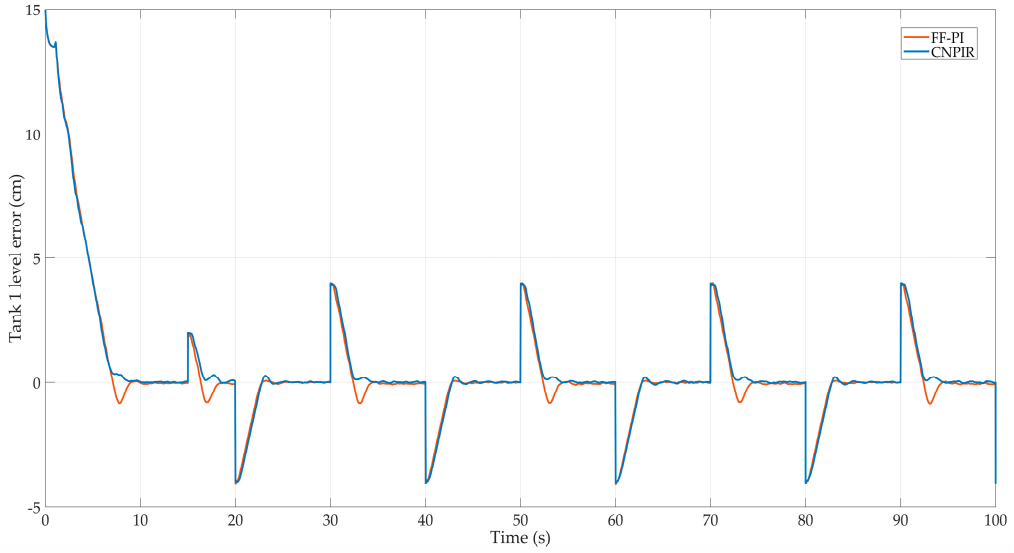

Figure 7. Tracking error for Tank 1 configuration.

To demonstrate the effectiveness of the proposed CNPIR controller compared to the FF-PI control, the integral square error (ISE) values, as formulated in Equation (31), were calculated. In this article, the control capability of the system was compared based on the integral square error, considering the changes in the h delay parameter, the application of the disturbance, and the duration of the disturbance.

$$ISE = \int_0^t e(t)^2 \, dt \tag{31}$$

The ISE error values of the graph obtained in Figure 7, comparing the control controllers without applying any disturbance to the system, are provided in Table 3. As seen, a lower ISE error value was achieved with the proposed CNPIR control technique. The ISE error values obtained for the designed system with the CNPIR controller, according to the changes in the h delay parameter, are provided in Table 4. The results show that the ISE error value increases significantly when the h delay parameter exceeds 200 milliseconds. It was concluded that the increase in error value is related to the system's response time.

Table 3. ISE values without disturbance according to controllers for Tank 1.

	FF-PI	CNPIR
ISE	630	552.9

Table 4. ISE values according to CNPIR h parameter change.

Controller	h value	ISE
CNPIR	2 ms	552.9
CNPIR	10 ms	552.5
CNPIR	90 ms	552.7
CNPIR	100 ms	557.2
CNPIR	200 ms	577.4

 doi:10.20944/preprints202408.0288.v1

CNPIR	300 ms	596.7
CNPIR	1 s	694.1

In order to prove that the CNPIR control method can perform better than the FF-PI controller, a liquid level position control experiment was conducted and compared. It was observed that the CNPIR controller could follow the reference better without overshoot and had better steady-state error performance compared to the FF-PI controller. The signals for the CNPIR and FF-PI controllers were obtained, as shown in Figure 8.

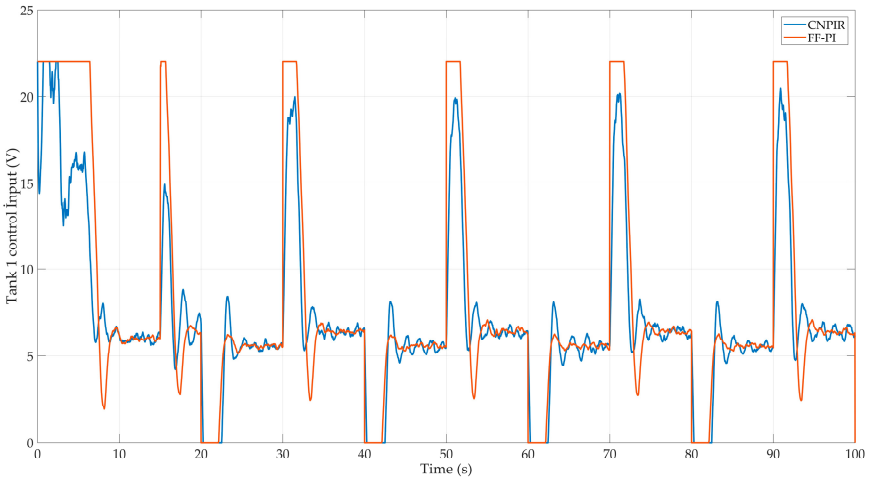

Figure 8. Tank 1 level control signs.

In order to evaluate the performance of the CNPIR and FF-PI controllers against instantaneous disturbances, instantaneous disturbances of different durations and intervals were applied in the experimental setup. To apply these disturbances, the external outlet valve located at the bottom of Tank 1, as shown in Figure 9, was used.

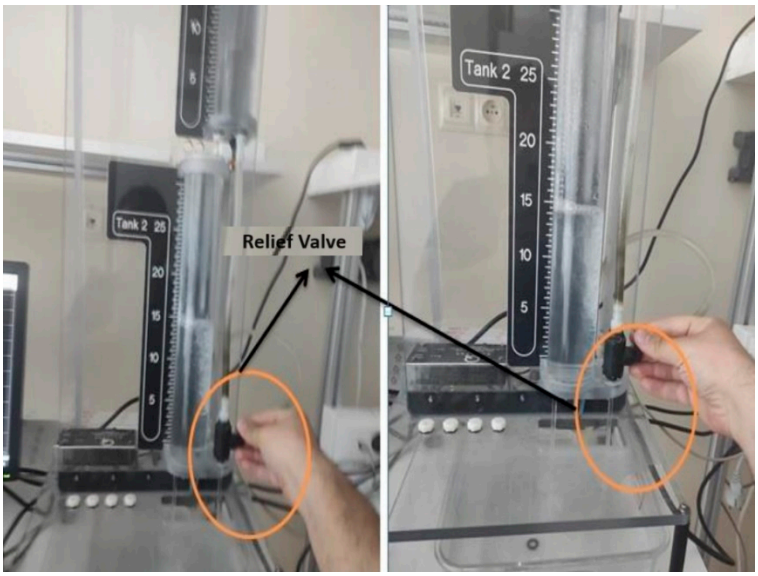

Figure 9. Tank-1 liquid level control giving instant disturbance effect.

In order to get the response of the proposed controller technique to undesirable situations, the system's drainage tap was opened every 10 seconds by external intervention into the system, as seen in Figure 9. This valve was fully opened for 10 seconds in each interval shown in Figure 10, causing

 doi:10.20944/preprints202408.0288.v1

the liquid level in Tank 1 to suddenly decrease. Since the amplitude and magnitude of the suddenly changing disturbance could not be directly measured, this situation became an unmeasurable disturbance for the system.

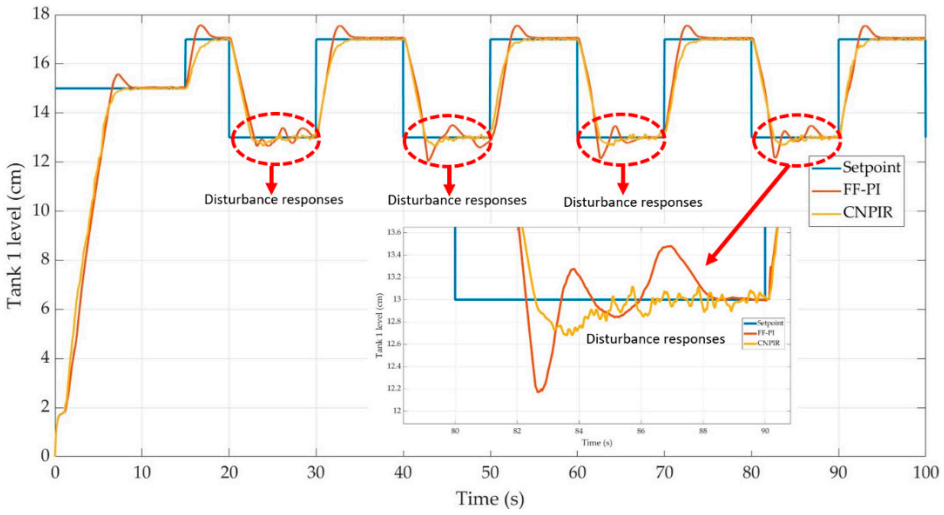

Figure 10. Square wave responses during disturbance for Tank 1 configuration.

As shown in Figure 10, the response of the Tank 1 control system to the applied disturbance, based on the ISE error values obtained from the control controllers, is provided in Table 5.

Table 5. ISE values with disturbance according to controllers for Tank 1.

	FF-PI	CNPIR
ISE	638.3	579.3

It is evident that the CNPIR controller performs better than the FF-PI control controller against disturbances applied at different durations and intervals. Against disturbances, the CNPIR controller exhibited less oscillation and responded faster to the system. Furthermore, its ability to follow the reference signal without overshooting proves its superior performance compared to the FF-PI controller. As seen in Figure 10, during disturbances lasting 10 seconds in each interval, the CNPIR controller generated control signals to quickly bring the liquid level close to the reference value by minimizing the error and forcing the system to stay at the reference value. When the duration and interval of the disturbance, as shown in Figure 10, are increased, it is concluded that the CNPIR control controller responds better to disturbances compared to the FF-PI controller. Examining the obtained graphs and the ISE error values, it was concluded that the proposed CNPIR control technique can control the liquid level in Tank 1 better than the FF-PI controller.

3.2. Results of Tank 2

Finally, we apply the same step trajectory to Tank 2 to showcase the performance of the proposed controller. In this setup, Tank 1's controller calculates the reference level, and Tank 2's controller is what determines the pump voltage command to ensure that the actual liquid level follows the given reference. As shown in Figures 11–13, the proposed CNPIR controller provides a rapid response with minimal overshoot and precise trajectory tracking compared to the FF-PI controller. Similarly, real-time results indicate that the proposed controller performs well for the Tank 2 configuration. Table 6 presents the optimal controller parameters for Tank 2, determined through experimentation.

Preprints.org (www.preprints.org) | NOT PEER-REVIEWED | Posted: 5 August 2024 doi:10.20944/preprints202408.0288.v1

Table 6. Liquid level Tank 2 system parameters.

FF-PI parameters		
K_{p_2}= 5.09	K_{i_2} = 1.74	K_{ff_2}= 1
CNPIR control parameters		
Square Wave G= 1.02	h=0.1 K_p= 10	K_i= 0.3 K_{ir}= 0.6

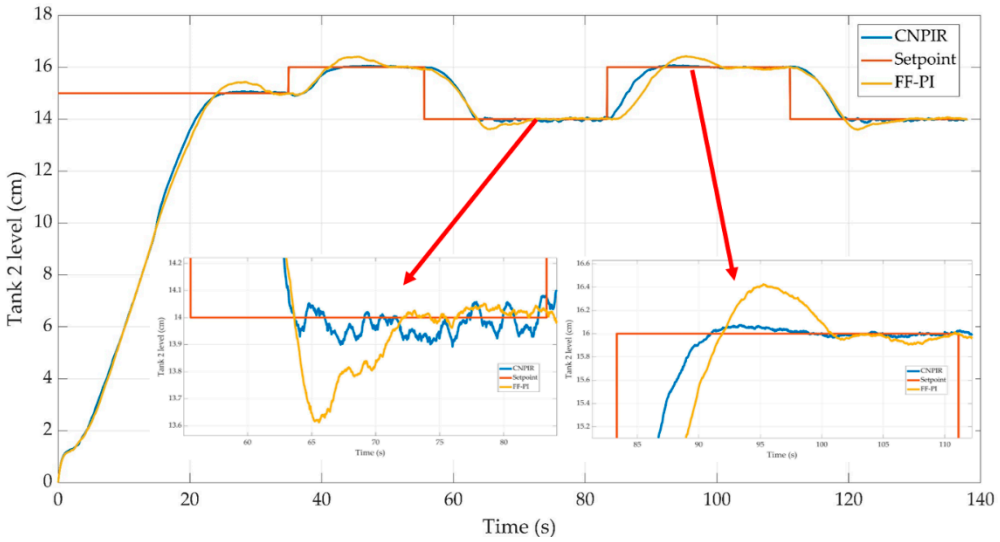

Figure 11. Control performances of the CNPIR and FF-PI controllers for Tank 2.

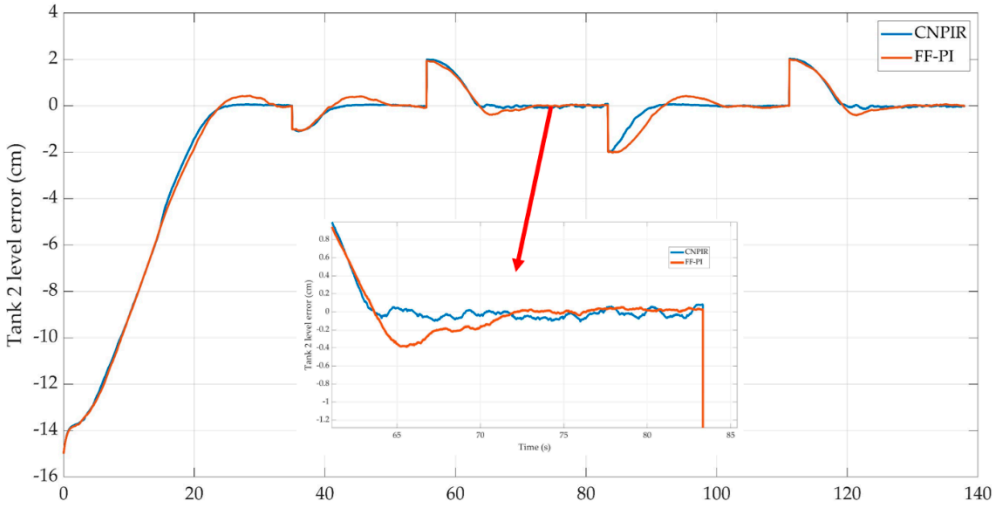

Figure 12. Tracking error for Tank 2 configuration.

 doi:10.20944/preprints202408.0288.v1

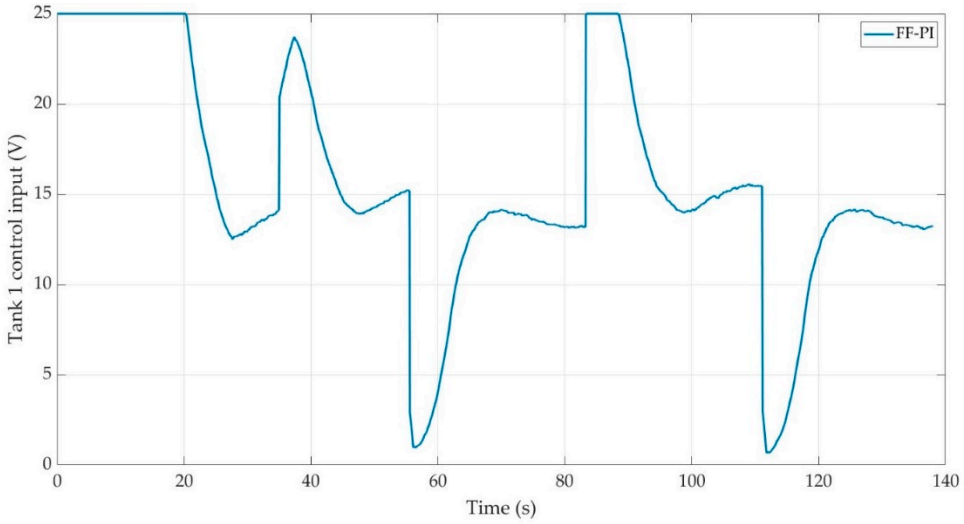

Figure 13. a. Control input for Tank 2 configuration (FF-PI).

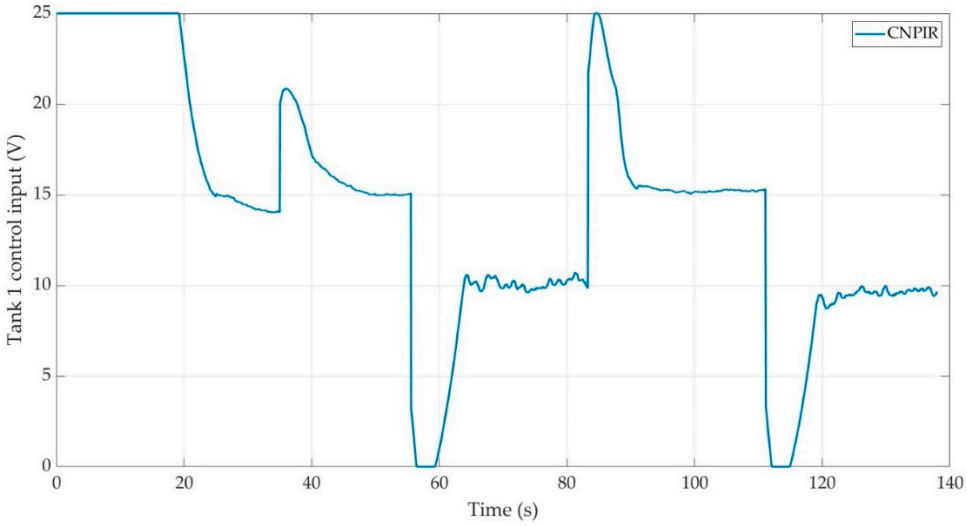

Figure 13. b. Control input for Tank 2 configuration (CNPIR).

As can be seen in Figures 11 and 12, the proposed CNPIR method exhibited better performance than FF-PI. The percentage overshoot value (Mp) was 0.47% in CNPIR, while it was 2.65% in FF-PI. The settling time (Ts) was 27.4 sec in CNPIR, while it was 32.98 sec in FF-PI. To demonstrate the effectiveness of the proposed CNPIR controller compared to the FF-PI control, the integral square error (ISE) values, as formulated in Equation (30), were calculated for Tank 2. The ISE error values of the graph obtained in Figure 12, are provided in Table 7. As can be seen from Table 7, lower ISE values are obtained in CNPIR due to the robust control signal of the CNPIR controller shown in Figure 13(b).

Table 7. ISE values for Tank 2.

	FF-PI	**CNPIR**
ISE	1743	1604

4. Discussion

In the proposed study, the cascade nonlinear feedforward proportional retarted controller has been applied to an industrial process system in real-time for the first time in the literature. A dynamic

analysis of the liquid level system was conducted, and different control methods were utilized to enhance the system's position control performance. Initially, the FF-PI controller was tested for the liquid level system. Later, the dynamic modelling of the control system was fully considered, and the CNPIR control technique, which is based on delay, was used. According to the results obtained from the real-time speed and position control experiments, although the classical PI controller is easy to implement, it is quite weak in terms of control performance. However, when an accurate dynamic model of the system is determined and used, particularly in the CNPIR control method, the control performance of the system is seen to be strengthened. The proposed controller's performance was observed to produce smoother signals and greater control accuracy compared to the FF-PI controller in real-time operations. Additionally, the CNPIR controller demonstrated excellent performance against time-varying references and sudden external disturbances. Future studies will include applying the proposed CNPIR controller to more complex systems with multiple degrees of freedom that have a known dynamic model. Furthermore, it is planned to apply the proposed control method to systems with fractional-order differential models.

Author Contributions: Conceptualization, K.K.A., A.D.; methodology, A.D., K.K.A.; software, A.D. and K.K.A.; validation, A.D., K.K.A., S.G. and E.T.; formal analysis, A.D. and K.K.A.; investigation, A.D and K.K.A.; data curation, A.D. and G.K.; writing—original draft preparation, A.D. and K.K.A.; writing—review and editing, K.K.A. and A.D.; visualization, K.K.A. and A.D; supervision, A.D.; project administration, A.D. and K.K.A.; funding acquisition, K.K.A. All authors have read and agreed to the published version of the manuscript.

Data Availability Statement: The supporting data of this article will be made available by the authors on request.

Conflicts of Interest: The authors declare no conflicts of interest.

References

1. Roy, A.; Iqbal, K. PID Controller Tuning for the First-Order-plus-Dead-Time Process Model via Hermite-Biehler Theorem. *ISA Transactions* **2005**, *44*, 363–378. https://doi.org/10.1016/S0019-0578(07)60210-9.
2. Munro, N. The Systematic Design of PID Controllers Using Nyquist Stabiliy. In Proceedings of the 2001 European Control Conference (ECC); IEEE: Porto, Portugal, September 2001; pp. 528–533.
3. Chen, D.; Seborg, D.E. Robust Nyquist Array Analysis Based on Uncertainty Descriptions from System Identification. *Automatica* **2002**, *38*, 467–475. https://doi.org/10.1016/S0005-1098(01)00207-2.
4. Nesimioğlu, B.S. Düşük Mertebeden Zaman Gecikmeli Sistemlerin Oransal Kontrolörler İle Kararlı Kılınması. 2016.
5. Tallman, G.; Smith, O. Analog Study of Dead-Beat Posicast Control. *IRE Trans. Automat. Contr.* **1958**, *4*, 14–21. https://doi.org/10.1109/TAC.1958.1104844.
6. Suh, I.; Bien, Z. Proportional Minus Delay Controller. *IEEE Trans. Automat. Contr.* **1979**, *24*, 370–372. https://doi.org/10.1109/TAC.1979.1102024.
7. Abdallah, C.; Dorato, P.; Benites-Read, J.; Byrne, R. Delayed Positive Feedback Can Stabilize Oscillatory Systems. In Proceedings of the 1993 American Control Conference; IEEE: San Francisco, CA, USA, June 1993; pp. 3106–3107.
8. Niculescu, S.-I.; Michiels, W. Stabilizing a Chain of Integrators Using Multiple Delays. *IEEE Trans. Automat. Contr.* 2004, *49*, 802–807. https://doi.org/10.1109/TAC.2004.828326.
9. Galip Ulsoy, A. Time-Delayed Control of SISO Systems for Improved Stability Margins. *Journal of Dynamic Systems, Measurement, and Control* **2015**, *137*, 041014. https://doi.org/10.1115/1.4028528.
10. Nalbantoğlu, M.; Yavuz G. SSSC tabanlı kaskad kontrolör ile güç sistem kararlılığının iyileştirilmesi. *Dicle Üniversitesi Mühendislik Fakültesi Mühendislik Dergisi* 8.1 2017; pp 89-100.
11. Xu, T.; Yu, H.; Yu, J.; Meng, X. Adaptive Disturbance Attenuation Control of Two Tank Liquid Level System With Uncertain Parameters Based on Port-Controlled Hamiltonian. *IEEE Access* 2020, *8*, 47384–47392. https://doi.org/10.1109/ACCESS.2020.2979352.
12. Sundaravadivu, K.; Arun, B.; Saravanan, K. Design of Fractional Order PID Controller for Liquid Level Control of Spherical Tank. In Proceedings of the 2011 IEEE International Conference on Control System, Computing and Engineering; IEEE: Penang, Malaysia, November 2011; pp. 291–295.
13. Gouta, H.; Said, S.H.; Barhoumi, N.; M'Sahli, F. Observer-Based Backstepping Controller for a State-Coupled Two-Tank System. *IETE Journal of Research* **2015**, *61*, 259–268. https://doi.org/10.1080/03772063.2015.1018846.

 doi:10.20944/preprints202408.0288.v1

14. Liang, L. The Application of Fuzzy PID Controller in Coupled-Tank Liquid-Level Control System. In Proceedings of the 2011 International Conference on Electronics, Communications and Control (ICECC); IEEE: Ningbo, China, September 2011; pp. 2894–2897.
15. Lian, S.T.; Marzuki, K.; Rubiyah, Y. Tuning of a Neuro-Fuzzy Controller by Genetic Algorithms with an Application to a Coupled-Tank Liquid-Level Control System. *Engineering Applications of Artificial Intelligence* **1998**, *11*, 517–529. https://doi.org/10.1016/S0952-1976(98)00012-8.
16. López, K.; Garrido, R.; Mondié, S. Cascade Proportional Integral Retarded Control of Servodrives. *Proceedings of the Institution of Mechanical Engineers, Part I: Journal of Systems and Control Engineering* **2018**, *232*, 662–671. https://doi.org/10.1177/0959651818767774.
17. Ranganayakulu, R.; Seshagiri Rao, A.; Uday Bhaskar Babu, G. Analytical Design of Fractional IMC Filter – PID Control Strategy for Performance Enhancement of Cascade Control Systems. *International Journal of Systems Science* **2020**, *51*, 1699–1713. https://doi.org/10.1080/00207721.2020.1773571.
18. Begum, K.G. Design of a Simple Control Strategy for Time-Delayed Unstable Series Cascade Processes. *Arab J Sci Eng* **2022**, *47*, 6679–6691. https://doi.org/10.1007/s13369-022-06650-7.
19. Yin, C.; Wang, H.; Sun, Q.; Zhao, L. Improved Cascade Control System for a Class of Unstable Processes with Time Delay. Int. J. Control Autom. Syst. 2019, 17, 126–135. https://doi.org/10.1007/s12555-018-0096-8.
20. Gao, J.; Xu, X.; Li, X.; Zhang, J.; Zhang, Y.; Wei, G. Model-Based Space Temperature Cascade Control for Constant Air Volume Air-Conditioning System. Building and Environment 2018, 145, 308–318. https://doi.org/10.1016/j.buildenv.2018.09.034.
21. Mao, J.; Yang, Z.; Zhang, S. Simulation of Liquid Level Cascade Control System Based on Genetic Fuzzy PID. In Proceedings of the 2022 5th International Conference on Robotics, Control and Automation Engineering (RCAE); October 2022; pp. 40–44.
22. Alfaro, V.M.; Vilanova, R.; Arrieta, O. Two-Degree-of-Freedom PI/PID Tuning Approach for Smooth Control on Cascade Control Systems. In Proceedings of the 2008 47th IEEE Conference on Decision and Control; December 2008; pp. 5680–5685.
23. Dogruer, T. Grey Wolf Optimizer-Based Optimal Controller Tuning Method for Unstable Cascade Processes with Time Delay. *Symmetry* **2022**, *15*, 54. https://doi.org/10.3390/sym15010054.
24. Dumlu, A.; Ayten, K.K. A Combined Control Approach for Industrial Process Systems Using Feed-Forward and Adaptive Action Based on Second Order Sliding Mode Controller Design. *Transactions of the Institute of Measurement and Control* **2019**, *41*, 1160–1171. https://doi.org/10.1177/0142331218790121.